Journal of Computational and Applied Mathematics 232 (2009) 82–89

Contents lists available at ScienceDirect

Journal of Computational and Applied Mathematics

journal homepage: www.elsevier.com/locate/cam

# On dependence of dynamical structure of numerical solutions of fluid simulations on forcibly added randomness

Itaru Hataue

*Graduate School of Natural Science and Technology, Kanazawa University, Kakuma-machi, Kanazawa, Ishikawa, 920-1192, Japan*

ARTICLE INFO

*Article history:*
Received 30 July 2007
Received in revised form 11 December 2007

*Keywords:*
Numerical simulation
Incompressible Navier–Stokes equations
Numerical error
Randomness
Asymptotic behavior of solutions
Stability

ABSTRACT

In the present paper, the dependencies of the numerical results of fluid simulations on forcibly added randomness are discussed. The incompressible Navier–Stokes equations and the continuity equation are solved numerically by using the MAC (Maker-And-Cell) method and implicit temporal scheme. The model adopted in the present study is a flow around a two-dimensional circular cylinder and the Reynolds number is 1500. The randomness which is given by using the pseudo-random number is forcibly added in the time marching step of the discretized Navier–Stokes equations. Dependencies of the averaged structure of asymptotic numerical solutions on the randomness are discussed. Furthermore, the dependence of the qualitative structure of the asymptotic solution of each sample calculation on the amplitude of randomness is also studied. It is clarified that forcibly added random errors may cover the nonlinear errors which make the system unstable.



## 1. Introduction

The complicated phenomena such as flow motions have been able to be simulated easily as if they were open before our eyes actually by modern computer systems and graphic tools. However, nobody can confirm whether computed results are reliable or not for the nonlinear cases in which true solutions of the original differential equations are not given. For example, it is well-known that the complicated flow motions are numerically given in the cases of the low Reynolds numbers, where the flows are expected to be physically laminar. The solutions which do not correspond to the true ones are often called spurious solutions or ghost ones and they have been studied in detail by a lot of researchers [1–6]. The author also studied the structure of the ghost solutions which appear in the fluid simulations on the basis of the concept that the system of numerical simulation is the nonlinear dynamical system [7–10]. Though the approximate conditions of calculations are set to be physically reasonable and the most suitable schemes to obtain reasonable results are selected, we found that there it is possible to get multiple approximately obtained invariant sets (attractors) in those reports. In particular, we studied the effect of the higher order artificial viscosity terms which are added explicitly and implicitly in some upwind schemes. As a result, we got several types of complicated spurious solutions even when we used the high order accurate upwind schemes which included the higher order artificial viscosity terms. Furthermore, we concluded that only selecting smaller $\Delta t$ values is not enough to get reasonable results [11].

There is another standpoint that the ghost solutions are produced by numerical errors. It is apprehended that several types of errors stabilize or destabilize the computing system. In order to realize what happens in numerical simulations, we studied numerical solutions of the stochastic difference equations (SDE's) on the assumption that the insertion processes of the errors are random. A simple example is the stochastic differential equation (SDE), based on the deterministic logistic

*E-mail address:* hataue@is.t.kanazawa-u.ac.jp.

0377-0427/$ – see front matter © 2008 Elsevier B.V. All rights reserved.
doi:10.1016/j.cam.2008.10.042

differential equation which was considered, and the relation between the size of noise and characteristics of obtained numerical solutions were discussed [12,13]. It was elucidated that relatively large random errors change the characteristics of attractors. In these cases, the added randomness may bring other unknown types of nonlinear stabilities and the qualitative statistical structure of the asymptotic numerical solutions changes. In practical fluid simulations, we have sometimes obtained stable spurious solutions in using rough numerical schemes. One of purposes of the present work is to clarify the dependence of the structure of numerical solutions on the randomness in the practical fluid simulations. Concretely, we adopted a flow around a circular cylinder as a simple model and discussed the dependence of the statistical structure on the amplitude of randomness by comparing the data reconstructed from the long period of time series of $C_d$ (drag coefficient) by applying the nonlinear dynamics approaches.

The numerical scheme used in the present paper is expressed briefly in Section 2. Other conditions of computations such as the grid systems, boundary conditions and so on are also described in Section 2. In Section 3, the dependence of the structure of the numerical solutions of the practical fluid simulations on the forcibly added randomness is discussed in detail.

## 2. Numerical algorithm and numerical conditions

### 2.1. Basic equations

The non-dimensional incompressible Navier–Stokes equations and the continuity equation are given as follows:

$$\begin{cases} \mathrm{div}\mathbf{V} = 0 \\ \dfrac{\partial \mathbf{V}}{\partial t} + (\mathbf{V}\cdot\mathrm{grad})\mathbf{V} = -\mathrm{grad}p + \dfrac{1}{Re}\Delta\mathbf{V} \ (+\ rR), \end{cases} \tag{1}$$

where $\mathbf{V} = (u, v)$, $p$ and $Re$ denote velocity vector, pressure and the Reynolds number, respectively. The term $R$ is the forcibly added randomness and $r$ is the parameter which denotes the strength of randomness. Randomness is given by using pseudo-random number.

### 2.2. Numerical algorithm

The Poisson equation for pressure can be derived on the basis of MAC method [14].

$$\Delta p = -\mathrm{div}(\mathbf{V}\cdot\mathrm{grad})\mathbf{V} + D, \tag{2}$$

where

$$D = -\frac{\partial \mathrm{div}\mathbf{V}}{\partial t} + \frac{1}{Re}\Delta\mathrm{div}\mathbf{V}. \tag{3}$$

In the present study, we employed the generalized transformation of coordinates, $(x, y) \rightarrow (\xi, \eta)$, then we get the transformed Poisson equation as follows:

$$\Delta p = -\frac{(y_\eta u_\xi - y_\xi u_\eta)^2 + 2(x_\xi u_\eta - x_\eta u_\xi)(y_\eta v_\xi - y_\xi v_\eta) + (x_\xi v_\eta - x_\eta v_\xi)^2}{J^2} - \frac{y_\eta u_\xi - y_\xi u_\eta + x_\xi v_\eta - x_\eta v_\xi}{J\Delta t}, \tag{4}$$

where $J$ is the Jacobian of transformation. The Poisson equation is solved using Gauss-Seidel scheme. All spatial derivatives except for those of the nonlinear convection term are discretized by using the central finite difference. For those of the convection terms, we considered parameter $\varepsilon$ in order to discuss the effects of fourth order artificial viscosity term based on the third-order upwind schemes [15],

$$f\frac{\partial u}{\partial \xi} = \frac{f_i(-u_{i+2} + 8u_{i+1} - 8u_{i-1} + u_{i-2})}{12\Delta\xi} + \varepsilon\frac{|f_i|(u_{i+2} - 4u_{i+1} + 6u_i - 4u_{i-1} + u_{i-2})}{4\Delta\xi^4}. \tag{5}$$

Viscous terms in Eq. (1) are discretized by using the second order central difference scheme. For the time marching of the Navier–Stokes equations, the first order backward Euler implicit scheme is employed. In the present implicit scheme, the nonlinear convection term is linearized for $\mathbf{V}^{n+1}$ as follows:

$$\left(\mathbf{V}^{n+1}\cdot\nabla\right)\mathbf{V}^{n+1} \approx \left(\mathbf{V}^{n}\cdot\nabla\right)\mathbf{V}^{n+1}. \tag{6}$$

Simultaneous equations of the linearlized implicit scheme are also solved using Gauss-Seidel method.

### 2.3. Grid systems

The O-type grid systems are used in all cases. The body surface corresponds to $K = 1$, the circle of which radius is equal to 1. Outer flow region corresponds to $K = KMAX$, the circle of which radius is set to from 60 to 70. The mesh points are

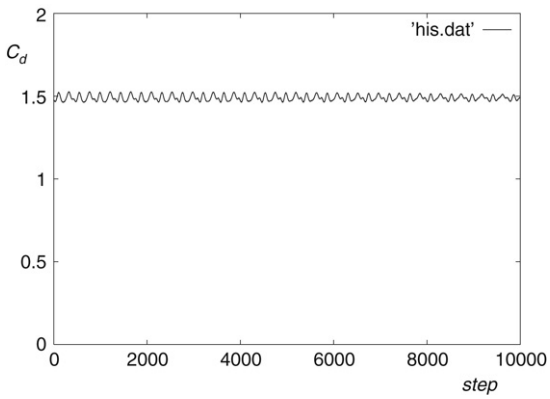


(a) Averaged time series, $r = 10^{-4}$.

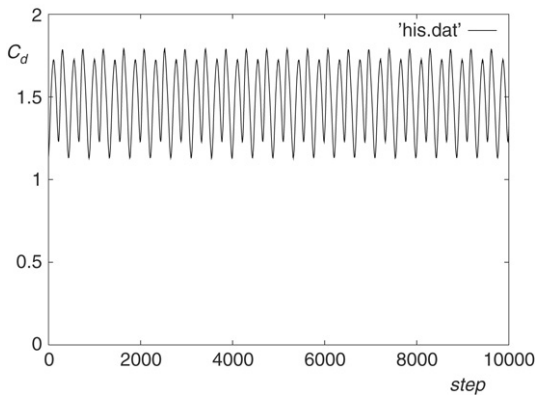


(b) One of the sample data, $r = 10^{-4}$.

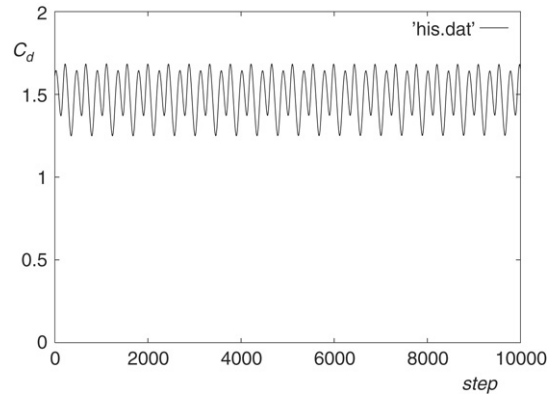


(c) Averaged time series, $r = 10^{-5}$.

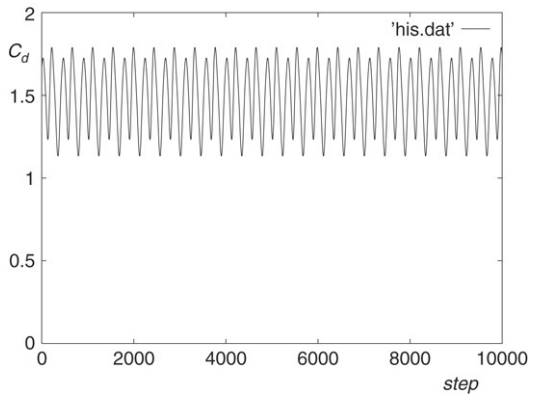


(d) One of the sample data, $r = 10^{-5}$.

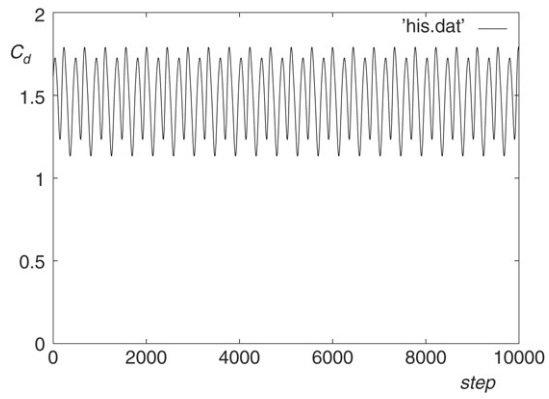


(e) $r = 0$.

**Fig. 1.** Comparisons of the profiles of the time series of $C_d$.

strongly concentrated in the boundary layer and the minimum spacing normal to the surface of the body is set to be less than $\frac{0.049}{\sqrt{Re}}$. Therefore this grid system is fine enough to resolve the flow structure in the boundary layer.

### *2.4. Boundary conditions*

The boundary conditions on the body surface are as follows: The no-slip condition is used for the velocity components. The pressure $p$ along the body surface is obtained by solving a normal momentum equation. At the far boundaries, the free-stream values are specified.

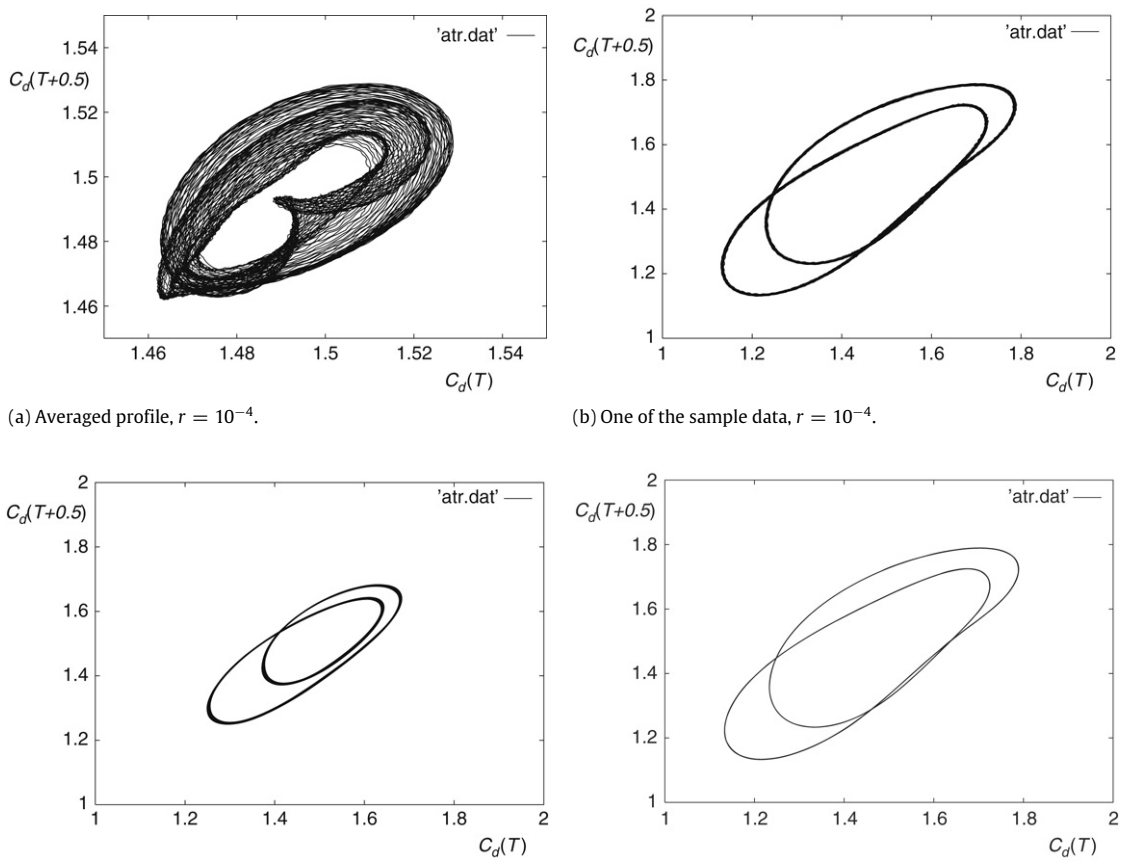


(a) Averaged profile, $r = 10^{-4}$.

(b) One of the sample data, $r = 10^{-4}$.

(c) Averaged profile, $r = 10^{-5}$.

(d) One of the sample data, $r = 10^{-5}$.

**Fig. 2.** Comparisons of the trajectories reconstructed on two-dimensional phase-plane.

## 3. Results and discussion

### 3.1. Statistical structure

In this subsection, we discuss the dependence of the statistical structure of numerical solutions of fluid simulations on insertion of random errors in detail. In calculations of averaged structure, we computed about 40 sample calculations in which different pseudo-random number rows are used throughout each calculation. The $\varepsilon$ value of the fourth order viscosity term is 2.0. Fig. 1 shows comparisons of profiles of time series of $C_d$ in the cases of $r$ (the strength of randomness) $= 10^{-4}$ and $10^{-5}$. $C_d$ values are estimated numerically by calculating the drag $D = \oint_c p dy$, where $c$ is the surface of the circular cylinder. The averaged time series which are given from all sampling data are shown (Fig. 1-(a), (c)). Fig. 1-(b) and (d) are the time series of one of the sampling data in the period from $T$ (non-dimensional time) $=$ 1500 to 2000. We also show the time series of the calculation in the case of $r = 0$ (Fig. 1-(e)) for comparison. In the case of $r = 0$, the clear periodic structure of flow field can be seen. In Fig. 2, we also show the trajectories reconstructed two-dimensionally from the time series. These trajectories are reconstructed in the $(C_d(T),\ C_d(T+0.5))$ phase space from time series of $C_d$ in the period from $T$ (non-dimensional time) $=$ 1500 to 2000. The amplitude of the averaged time series in the case of $r = 10^{-4}$ is small and the profile is not periodic. In the case of $r = 10^{-5}$, the profiles looks periodic and the amplitude is a little smaller than that in the case of $r = 0$. On the other hand, the amplitudes of two sampling data ((b), (d)) are similar and the profiles of two-dimensional trajectories are almost periodic. Therefore, it is supposed that the time when the uniform flow becomes unstable and periodical structure occurs is affected by a weak randomness. However, once such periodic structure grows up, that system is not so influenced by the weak randomness.

### 3.2. Effect of the forcibly added randomness

In this subsection, we discuss the structure of each sample calculation in the cases in which the stabilizing fourth order viscosity terms ($\varepsilon$ values) are not so large. Therefore, the nonlinear instability is not negligible and there is a possibility to get the spurious solutions. At first, we show the comparisons of the profiles of two-dimensional trajectories in Fig. 3.

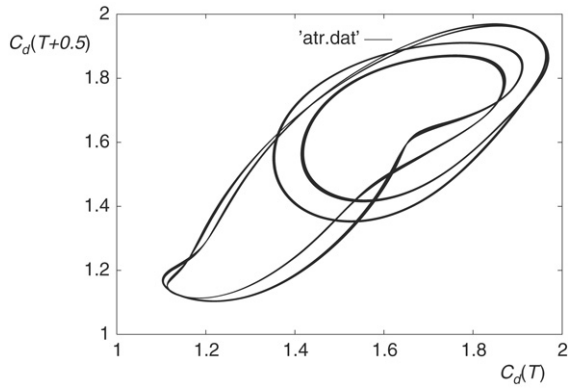


(a) $\varepsilon = 0.57, r = 0$.

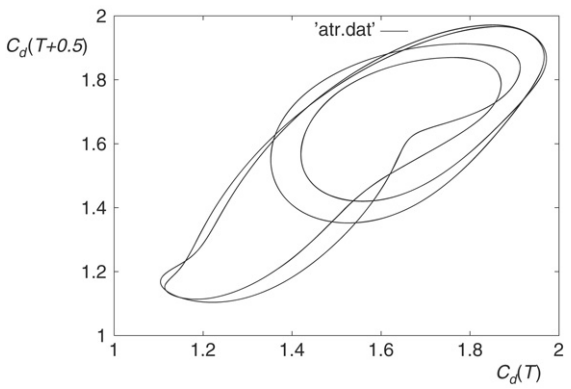


(b) $\varepsilon = 0.56, r = 0$.

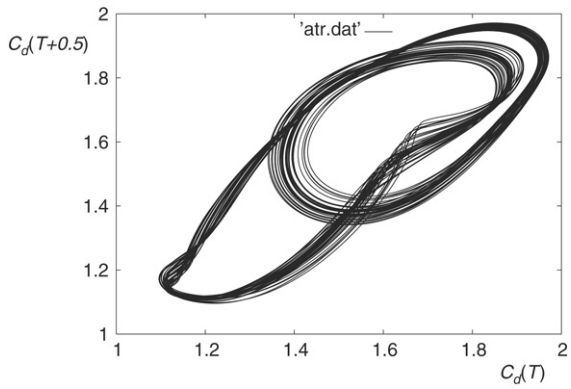


(c) $\varepsilon = 0.60, r = 0$.

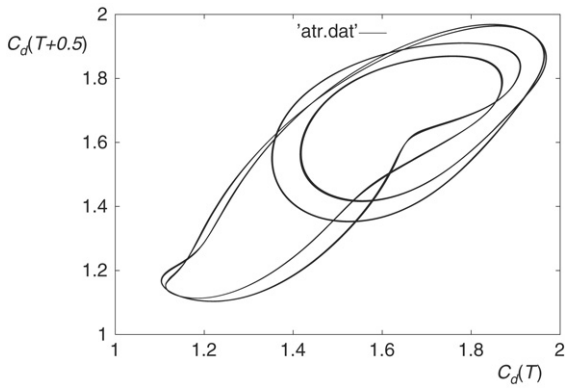


(d) $\varepsilon = 0.57, r = 10^{-5}$(A).

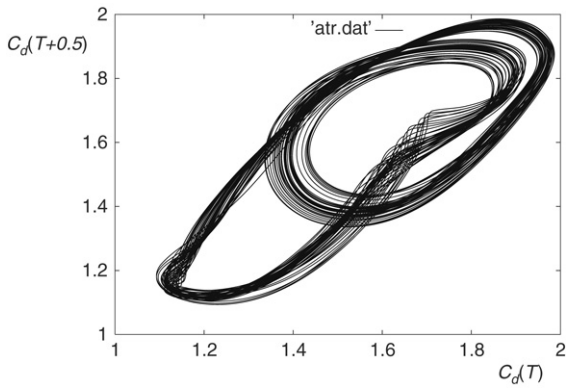


(e) $\varepsilon = 0.57, r = 10^{-5}$(B).

**Fig. 3.** Comparisons of the trajectories reconstructed on two-dimensional phase-plane.

In these region of $\varepsilon$ values, structure of the invariant sets is sensitive for the change of $\varepsilon$ values. Fig. 3-(d) and -(e) are two sampling data in the case of $r = 10^{-5}$. Fig. 3-(d) (sample(A)) and Fig. 3-(e) (sample(B)), which are given by using the different pseudo-random number rows, are similar to Fig. 3-(b) and -(c), respectively. This result shows that weak noises make the characteristic of the invariant set change and the effects of the noises are similar to those of the fourth viscosity terms. In Fig. 4, comparisons of the structure of typical sampling calculations which are given by using different pseudo-random number rows are shown by the power spectral density of the time series as a function of frequency. In two cases in which the random errors are forcibly added ($r = 2 \times 10^{-4}$), characteristic peaks which are caused by the forcibly added randomness can be seen in very high frequency region (Fig. 4-(f) and -(i)). On the other hand, the fine structures which are seen in the calculation without noises ($r = 0$: Fig. 4-(b)) disappear in two cases which include random noises (Fig. 4-(e) and -(h)). As for the profile of reconstructed trajectory, we can see the widely broadening profiles in Fig. 4-(a). Width of trajectory of

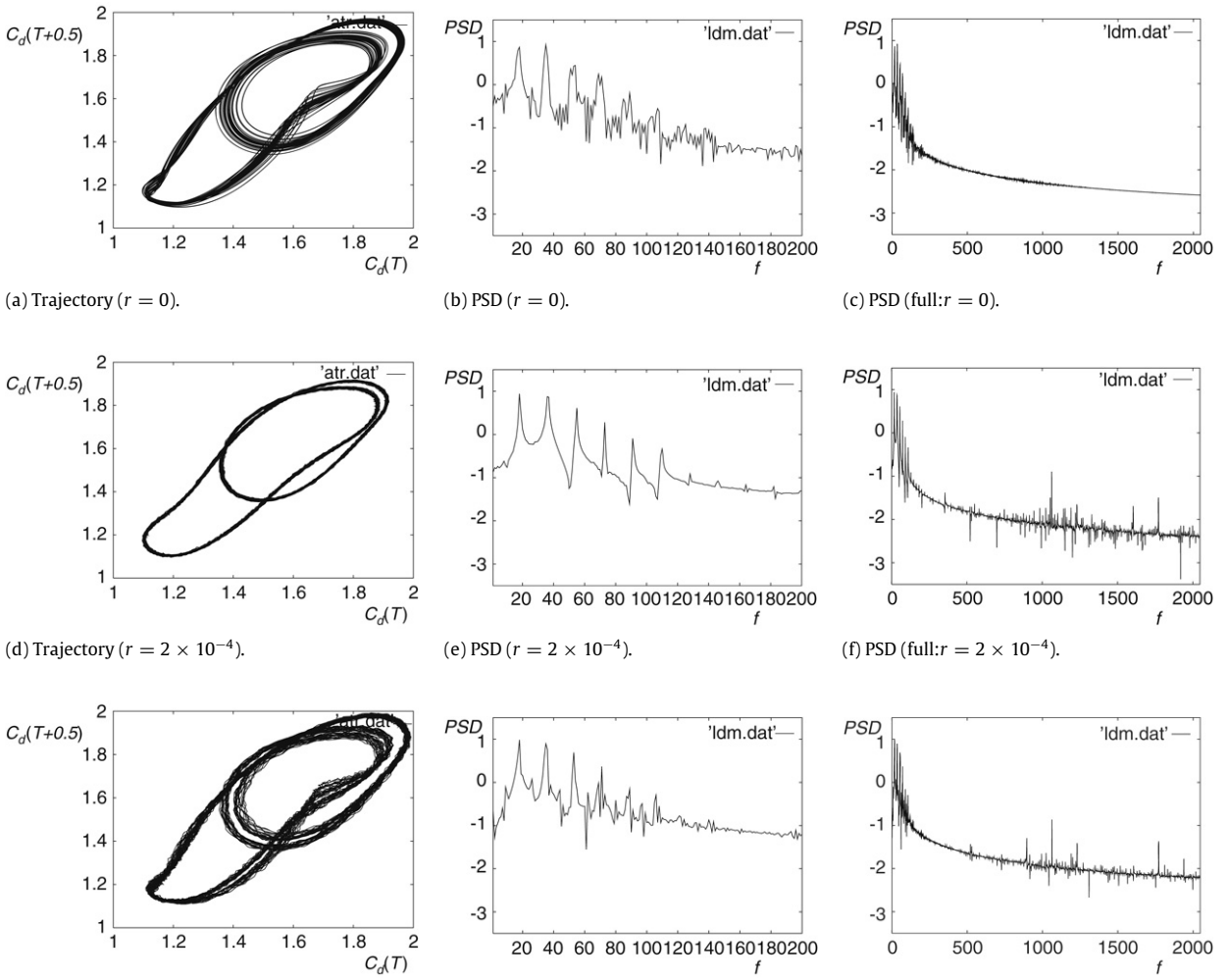


(a) Trajectory ($r = 0$). (b) PSD ($r = 0$). (c) PSD (full:$r = 0$).

(d) Trajectory ($r = 2 \times 10^{-4}$). (e) PSD ($r = 2 \times 10^{-4}$). (f) PSD (full:$r = 2 \times 10^{-4}$).

(g) Trajectory ($r = 2 \times 10^{-4}$). (h) PSD ($r = 2 \times 10^{-4}$). (i) PSD (full:$r = 2 \times 10^{-4}$).

**Fig. 4.** Comparisons of the structure of several sample calculations which show the effect of the forcibly added random noises.

Fig. 4-(d) looks narrower than that of Fig. 4-(a) and there is only a little wide peak and its harmonics can be seen in the profile of the power spectral density (Fig. 4-(e)). Furthermore, the broadening of band of periodic 4 can be seen in Fig. 4-(g) which is not seen in Fig. 4-(a). Because the system is stable in the case of $\varepsilon = 2.0$ in the Section 3.1, each sampling calculation has the almost the same structure. However, results in this subsection show that it happens that several types of asymptotic sampling results are obtained by the forcibly added random noises in the case of $\varepsilon = 0.61$.

Does the structure of the asymptotic solution change if we continued the calculation by removing noises after the nondimensional time of $T_r = 2000$? We show the profiles of trajectories of asymptotic solution without the forcibly added noises $T_r = 2000$ (a) and $T_r = 500$ (b) in Fig. 5. From $T = 0$ to $T_r$, calculations are performed by using the same pseudo-random number rows that is used throughout the calculation shown in Fig. 4-(d). Asymptotic numerical solutions without the noises after some points converge to the similar one shown in Fig. 4-(a). This result shows that the solutions of Fig. 4-(d) and -(g) are not stable and they are obtained under the condition to being restricted by the effect of random noises. However, we must realize that there is a possibility that the different asymptotical numerical solutions may be given by the insertion of the random noises. On the other hand, we compare profiles of trajectories of several asymptotic solutions which are given under the different times when we begin to add the noises in Fig. 6. Fig. 4-(d) is the trajectory given by being added the random noises throughout the calculation. Though we cannot find clear differences among the figures in Fig. 6, they are different from that of Fig. 4-(d). This result shows that the structure of the unstable asymptotic solution shown in Fig. 4-(d) may be determined in the very early stages of calculation.

## 4. Conclusion

In the present paper, the dependence of the unsteady structure of asymptotic numerical solutions of the incompressible Navier–Stokes equations on the randomness was discussed by comparing the dynamical structure of asymptotic numerical

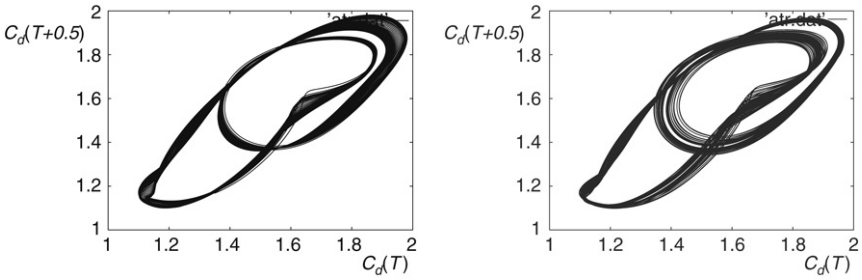


(a) Removed after $T = 2000$. (b) Removed after $T = 500$.

**Fig. 5.** Comparisons of the structure of several sample calculations which are given by removing the forcibly added random noises from in the middle of calculations.

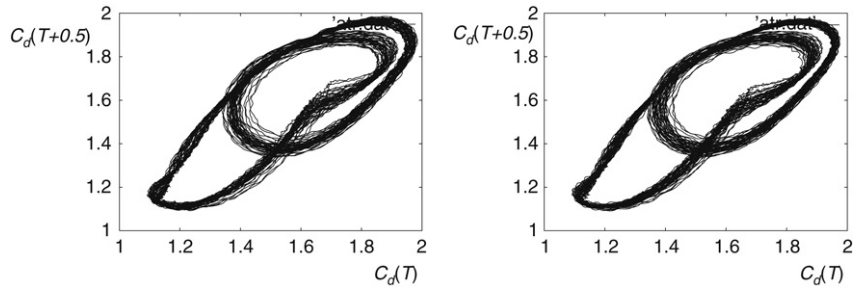


(a) Added after $T = 50$. (b) Added after $T = 100$.

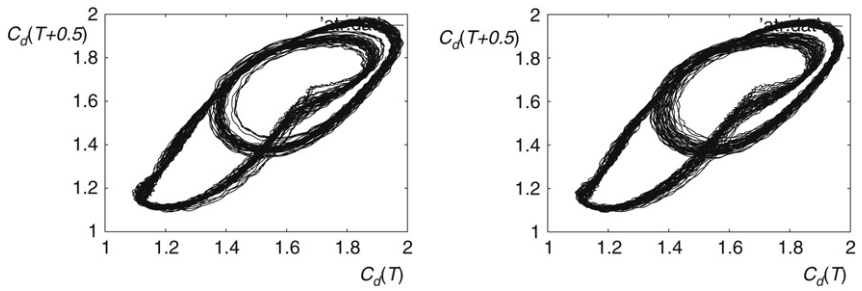


(c) Added after $T = 250$. (d) Added after $T = 500$.

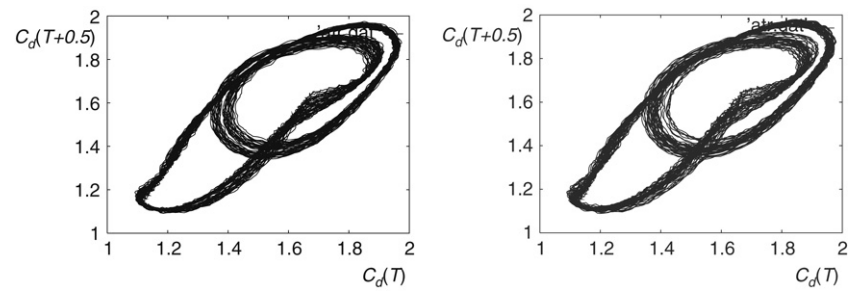


(e) Added after $T = 1000$. (f) Added after $T = 2000$.

**Fig. 6.** Comparisons of the structure of several sample calculations which are given by beginning to add the random noises in the middle of calculations.

solutions. In particular, we discussed the analogy of the numerical fourth order artificial viscosity term and the forcibly added randomness for the stabilizing effects by using nonlinear dynamics approaches. When the numerical fourth order artificial viscosity term is large, it is clarified that the time when the system becomes unstable and periodical structure occurances are affected by a weak randomness in each sample calculation. However, once such a periodic structure matures, the system is not so influenced by the weak randomness and the amplitude of averaged time series becomes small. On the other hand,

we studied the cases in which the stabilizing fourth order viscosity terms are not so large and the nonlinear instability is not negligible. It is clarified that weak noises make the system change and the effects of the noises are similar to those of the fourth viscosity terms. Then, a little large randomness gives several types of the lower-order invariant sets which are the spurious asymptotic solutions. These spurious solutions are unstable and the characteristics of these change easily by removing the forcibly added randomness. Furthermore, it is elucidated that the structure of these unstable asymptotic solutions may be determined in the very early stages of the calculation.

In the practical fluid simulations, several types of numerical errors are more or less inserted. The insertion processes of such numerical errors are usually random. If the system is stable, it may not be necessary to consider the influences of these numerical errors. However, we must take care of the dependencies of qualitative structure of numerical results of simulations on the effects of random errors for the unstable system. Researchers in the field of computational fluid dynamics should realize that the dependence of results of numerical simulations on the insertion of random errors is very serious. It is indispensable to study the dependencies of averaged structure and that of each sample calculation on the numerical random errors.

## Acknowledgments

This work was supported in part by the Grant-in-Aid for Scientific Research (C) of Japan Society for the Promotion of Science, No. 20540112.

## References

[1] A. Stuart, Nonlinear instability dissipative finite difference schemes, SIAM Rev. 31 (1989) 191–220.
[2] H.C. Yee, P.K. Sweby, D.F. Griffiths, Dynamical approach study of spurious steady-state numerical solutions of nonlinear differential equations. I. The dynamics of time discretization and its implications for algorithm development in computational fluid dynamics, J. Comput. Phys. 97 (1991) 249–310.
[3] D.F. Griffiths, P.K. Sweby, H.C. Yee, On spurious asymptotic numerical solutions of explicit Runge–Kutta methods, IMA J. Numer. Anal. 12 (1992) 263–290.
[4] A.R. Humphries, Spurious solutions of numerical methods for initial value problems, IMA J. Numer. Anal. 13 (1993) 263–290.
[5] M. Yamaguchi, S. Ushiki, Chaos in numerical analysis of ordinary differential equations, Physica C 3 (1981) 618–626.
[6] Y. Maeda, Euler's discretization revisited, Proc. Japan Acad. 71 (Ser A) (1995) 133–149.
[7] I. Hataue, Spurious numerical solutions in higher dimensional discrete systems, AIAA J. 33 (1995) 163–164.
[8] I. Hataue, Ghost numerical solutions in upwind difference scheme and effects of linearization, AIAA-Paper, 97–0870, 1997.
[9] I. Hataue, Mathematical and numerical analyses of dynamical structure of numerical solutions of two-dimensional fluid equations, J. Phys. Soc. Japan 67 (1998) 1895–1911.
[10] I. Hataue, On the structure of numerical solutions of flow simulation by implicit scheme, J. Phys. Soc. Japan 70 (2001) 1905–1911.
[11] I. Hataue, On analogy and dissimilarity of dependence of stability on several parameters in flow simulations, J. Comp. and Appl. Math. 159-1 (2003) 45–53.
[12] I. Hataue, On dependence of structure of numerical solutions on insertion of random errors, AIAA-Paper, 07–0107, 2007.
[13] I. Hataue, Y. Saisho, Effect of random errors on statistical behavior of discretized dynamical system, Information 10–1 (2007) 5–14.
[14] F.H. Harlow, J.E. Welch, Numerical calculation of time-dependent viscous incompressible flow of fluid with free surface, Phys. Fluids 8 (1965) 2182–2189.
[15] T. Kawamura, K. Kuwahara, Computation of high Reynolds number flow around a circular cylinder with surface roughness, AIAA Paper, 84–0340, 1984.